

# DNA-SIP reveals functional guild diversity and membership for labile and recalcitrant C decomposition in soil

Ashley N Campbell and Charles Pepe-Ranney \* † ‡, Chantal Koechli, Sean Berthrong, and Daniel H Buckley ‡

\*These authors contributed equally to the manuscript and should be considered co-first authors, †Department of Microbiology, Cornell University, New York, USA, and ‡Department of Crop and Soil Sciences, Cornell University, New York, USA

Submitted to Proceedings of the National Academy of Sciences of the United States of America

## Abstract

We identified microorganisms participating in xylose and/or cellulose decomposition in soil microcosms using nucleic acid stable isotope probing (SIP) coupled to next generation sequencing. 49 and 63 OTUs assimilated  $^{13}\text{C}$  from xylose and cel-  
lulose into DNA, respectively. Microorganisms as-  
similated xylose-C at days 1, 3, and 7. Cellulose-  
C assimilation peaked at day 14 and was main-  
tained at day 30. Many SIP-identified cellulose  
degraders are members of cosmopolitan but phys-  
iologically uncharacterized soil microbial lineages  
including *Spartobacteria*, *Chloroflexi* and *Planctomyces*.  $^{13}\text{C}$  from Xylose was initially assimilated by *Firmicutes* followed by *Bacteroidetes* and *Actionbacteria*. Trophic interactions may have caused  
this temporal pattern of incorporation. Soil C cy-  
cling models, however, often disregard bacterial  
trophic interactions. Fast growing substrate genera-  
lists assimilated xylose-C and slow growing sub-  
strate specialists assimilated cellulose-C. Xylose-  
C assimilators within time points clustered phylo-  
genetically, and cellulose-C assimilators clustered  
phylogenetically overall. Knowledge of soil C  
cycling functional guild diversity, membership and  
activity will improve the predictive power of ter-  
restrial C flux models.

stable isotope probing | structure-function relationships | soil mi-  
crobial ecology | 16S rRNA gene

Abbreviations: C, Carbon; OTU, Operational Taxonomic Unit; SOM,  
Soil Organic Matter; BD, Buoyancy Density; SIP, Stable Isotope Prob-  
ing

## Significance

We have a limited understanding of soil carbon (C) cycling yet soil contains a large fraction of the global C pool. Microorganisms mediate most soil C cycling but have proven difficult to study due to the complexity of soil C biochemistry and the wide range of soil microorganisms participating in C reactions. We demonstrate C use dynam-

ics by soil microbial taxa. Furthermore, we identi-  
fied microorganisms involved in cellulose decomposi-  
tion that were previously uncharacterized physi-  
ologically – cellulose is the most globally abundant  
biopolymer. Our results expand knowledge of soil  
functional guild diversity and activity which reveal  
soil structure-function relationships. This study is  
a departure from typical nucleic acid SIP studies  
that focus on listing the identities of heavy isotope  
labeled organisms. Our approach enables DNA-  
SIP to identify  $^{13}\text{C}$  labeled microorganisms with  
greater resolution producing a better sampling of  
functional guilds. This not only allows us to con-  
nect function to genetic identity but also allows  
us to assess functional guild diversity and uncover  
ecological strategies. Further, we demonstrate how  
substrate specificity can be assessed from DNA-  
SIP data.

## Introduction

Excluding plant biomass, there are 2,300 Pg of  
carbon (C) in soils worldwide which accounts for  
~80% of the global terrestrial C pool [1, 2]. Fungi,  
archaea, and bacteria degrade plant biomass that  
reaches soil respiration the majority of plant biomass  
C producing 10 times more  $\text{CO}_2$  annually than an-  
thropogenic emissions [3]. Rising atmospheric  $\text{CO}_2$   
may stimulate plant growth and in turn increase  
plant biomass C input to soil [4]. Current climate  
change models concur on atmospheric and oceanic,

## Reserved for Publication Footnotes

but not terrestrial, global C flux predictions [5]. Contrasting terrestrial C model predictions reflect how little is known about soil C cycling. We need to establish the roles and diversity of soil microbial community members involved with soil C cycling to reconcile inconsistencies in terrestrial C models [6, 7].

Functional guild membership and diversity establish the connections between soil functions and community structure [8]. Microorganisms mediate an estimated 80–90% of soil C cycling [9, 10] but the complexity of soil obfuscates microbial contributions to soil C cycling and the majority of microorganisms resist cultivation in the laboratory. Stable-isotope probing (SIP), however, links genetic identity and activity without cultivation and has expanded our knowledge of microbial contributions to biogeochemical processes [11]. Successful applications of SIP have identified organisms which mediate processes performed by functionally specialized microorganisms of limited diversity such as methanogens [12] but SIP has been less applicable in soil C cycling studies because simultaneous labeling of many different organisms has necessitated prohibitory resolving power. High throughput DNA sequencing technology, however, improves the resolving power of SIP enabling exploration of complex soil C-cycling processes.

This study aimed to observe labile C versus polymeric C assimilation dynamics in the soil microbial community. In soil microcosms we added a mixture of nutrients and C substrates that simulated the composition of plant biomass. All microcosms received the same C substrate mixture where the only difference between treatments was the identity of the isotopically labeled substrate. Specifically, we set up a series of microcosms with three treatments: in one treatment xylose was substituted for its  $^{13}\text{C}$ -equivalent, in another cellulose was substituted for its  $^{13}\text{C}$ -equivalent, and in the third treatment all substrates in the mixture were unlabeled. We harvested microcosms from each treatment at days 3, 7, 14 and 30 and additionally harvested microcosms receiving  $^{13}\text{C}$ -xylose and unlabeled substrates on day 1. We chose to label xylose and cellulose to contrast labile C and polymeric C decomposition, respectively. Post incubation, we sequenced 16S rRNA genes from SIP density fractions with high throughput DNA sequencing technology. Our experimental design allowed us to observe the soil microbial community members that assimilated xylose-C and cellulose-C over time.

## Results

Our experimental design allowed us to track the flow of xylose and cellulose C through the soil mi-

crobial community (Figure S1). 5.3 mg C substrate mixture per gram of soil was added to each microcosm representing 18% of the soil C. The mixture included 0.42 mg xylose-C and 0.88 mg cellulose-C per gram soil. Microcosms were harvested at days 1, 3, 7, 14 and 30 during a 30 day incubation.  $^{13}\text{C}$ -xylose assimilation peaked immediately and tapered over the 30 day incubation whereas  $^{13}\text{C}$ -cellulose assimilation peaked two weeks after amendment additions (Figure 1, Figure S2). See Supplemental Note XX for sequencing and density fractionation statistics. Microcosm treatments (see Methods) are identified in figures by the following code: “13CXPS” refers to the amendment with  $^{13}\text{C}$ -xylose ( $^{13}\text{C}$  Xylose Plant Simulant), “13CCPS” refers to the  $^{13}\text{C}$ -cellulose amendment and “12CCPS” refers to the amendment that only contained  $^{12}\text{C}$  (i.e. control).

**Soil microcosm microbial community changes with time.** Changes in the bulk soil microcosm microbial community structure and membership correlated significantly with time (Figure S3, P-value 0.23,  $R^2$  0.63, Adonis test [13]). The identity of the  $^{13}\text{C}$ -labeled substrate added to the microcosms did not significantly correlate with bulk soil community structure and membership (P-value 0.35). Additionally, microcosm beta diversity was significantly less than gradient fraction beta diversity (Figure S3, P-value 0.003, “betadisper” function R Vegan package [14, 15]). Twenty-nine OTUs significantly changed in relative abundance with time (“BH” adjusted P-value < 0.10, [16]) and of these 29 OTUs, 14 were found to incorporate  $^{13}\text{C}$  from labeled substrates into biomass (Figure S4). Four taxonomic classes significantly (adjusted P-value < 0.10) changed in abundance: *Bacilli* (decreased), *Flavobacteria* (decreased), *Gammaproteobacteria* (decreased) and *Herpetosiphonales* (increased) (Figure S5). Abundances grouped by phylum for OTUs that incorporated  $^{13}\text{C}$  from cellulose increased with time whereas abundances grouped by phylum of OTUs that incorporated  $^{13}\text{C}$  from xylose decreased over time although *Proteobacteria* abundance spiked at day 14 (Figure S6).

**OTUs that assimilated  $^{13}\text{C}$  into DNA.** Within the first 7 days of incubation 63% of  $^{13}\text{C}$ -xylose was respired and only 6% more was respired from day 7 to 30. At day 30, 30% of the  $^{13}\text{C}$  from xylose remained in the soil. An average 16% of the  $^{13}\text{C}$ -cellulose added was respired within the first 7 days, 38% by day 14, and 60% by day 30.

We refer to OTUs that putatively incorporated  $^{13}\text{C}$  into DNA originally from an isotopically labeled substrate as substrate “responders” (see Supplemental Note XX for operational “response” criteria). There were 19, 19, 15, 6, and 1  $^{13}\text{C}$ -

xylose responders at days 1, 3, 7, 14, 30, respectively (Figure S2). The numerically dominant  $^{13}\text{C}$ -xylose responder phylum shifted from *Firmicutes* to *Bacteroidetes* and then to *Actinobacteria* across days 1, 3 and 7 (Figure 2, Figure 3). *Proteobacteria*  $^{13}\text{C}$ -xylose responders were found at days 1, 3, 7 but peaked at day 7 (Figure 3).

Only 2 and 5 OTUs responded  $^{13}\text{C}$ -cellulose at days 3 and 7, respectively. At days 14 and 30, 42 and 39 OTUs responded to  $^{13}\text{C}$ -cellulose (Figure S2). *Proteobacteria*, *Verrucomicrobia*, and *Chloroflexi* had relatively high numbers of responders with strong response across multiple time points (Figure 2). *Verrucomicrobia*  $^{13}\text{C}$ -cellulose responders were 70% *Spartobacteria*. *Chloroflexi* responders were annotated as members of the *Herpetosiphonales* and *Anaerolineae* (Figure ??). *Celvibrio*, a canonical soil cellulose degrader, was found to respond strongly to  $^{13}\text{C}$ -cellulose in the microcosms. See Supplemental Note XX for further counts of  $^{13}\text{C}$ -responsive OTUs at greater taxonomic resolution.

**Ecological strategies of  $^{13}\text{C}$  responders.**  $^{13}\text{C}$ -xylose responders are generally more abundant members based on relative abundance in bulk DNA SSU rRNA gene content than  $^{13}\text{C}$ -cellulose responders (Figure 4, P-value 0.00028, Wilcoxon Rank Sum test). However,  $^{13}\text{C}$ -xylose and  $^{13}\text{C}$ -cellulose responders included both abundant and rare OTUs (Figure 4). Two  $^{13}\text{C}$ -cellulose responders were not found in any bulk samples (“OTU.862” and “OTU.1312”, Table S1). Of the 10 most abundant responders, 8 are  $^{13}\text{C}$ -xylose responders and 6 of these 8 are consistently among the 10 most abundant OTUs in bulk samples.

Cellulose-responder-DNA buoyant density (BD) shifted further along the density gradient than xylose-responder-DNA BD in response to  $^{13}\text{C}$  incorporation (Figure S7, Figure 4, P-value 1.8610x $^{-6}$ , Wilcoxon Rank Sum test).  $^{13}\text{C}$ -cellulose-responder-DNA BD shifted on average 0.0163 g mL $^{-1}$  (sd 0.0094) whereas xylose responder BD shifted on average 0.0097 g mL $^{-1}$  (sd 0.0094). For reference, 100%  $^{13}\text{C}$  DNA BD is 0.04 g mL $^{-1}$  greater than the BD of its  $^{12}\text{C}$  counterpart. DNA BD increases as its ratio of  $^{13}\text{C}$  to  $^{12}\text{C}$  increases. An organism that only assimilates C into DNA from a  $^{13}\text{C}$  isotopically labeled source, will have a greater  $^{13}\text{C}$  to  $^{12}\text{C}$  ratio in its DNA than an organism utilizing a mixture of isotopically labeled and unlabeled C sources (see Supplemental Note XX). We predicted the *rrn* gene copy number for each OTU as described previously [17]. The estimated *rrn* gene copy number for  $^{13}\text{C}$ -xylose responders was inversely related to time point of the first response for each OTU (P-value 2.02x10 $^{-15}$ , Figure S8). OTUs that did not

respond at day 1 respond but did respond at day 3 and/or day 7 had fewer estimated *rrn* copy number than OTUs that responded at day 1 (Figure S8).

We assessed phylogenetic clustering of  $^{13}\text{C}$ -responsive OTUs with the Nearest Taxon Index (NTI), the Net Relatedness Index (NRI), and the consenTRAIT metric [18]. Briefly, positive NRI and NTI with corresponding low P-values indicates deep phylogenetic clustering whereas negative NRI with high P-values indicates taxa are overdispersed compared to the null model [19]. NRI and P-values for substrate responder groups suggest  $^{13}\text{C}$ -xylose responders are overdispersed (NRI: -1.33, P: 0.90) while  $^{13}\text{C}$ -cellulose responders are clustered (NRI: 4.49, P: 0.001). NTI values show that both  $^{13}\text{C}$ -cellulose and  $^{13}\text{C}$ -xylose responders are clustered near the tips of the tree (NTI: 1.43 (P: 0.072), 2.69 (P: 0.001), respectively). The consenTRAIT clade depth for  $^{13}\text{C}$ -xylose and  $^{13}\text{C}$ -cellulose responders was 0.012 and 0.028 16S rRNA sequence dissimilarity, respectively.

## Discussion

**Microbial response to isotopic labels.** DNA-SIP can establish functional roles for thousands of phylogenotypes in a single experiment without cultivation. We identified 104 soil OTUs that incorporated  $^{13}\text{C}$  from xylose and/or cellulose into biomass over time. With this information we can build a conceptual model for the soil food web with respect to xylose and cellulose in our microcosms. We propose xylose and cellulose C added to soil microcosms took the following path through the microbial food web (Figure S9): fast-growing *Firmicutes* spore formers first assimilated xylose C within 24 hours. Over the next 6 days, biomass from early-responding *Firmicutes* and the remaining xylose-C and was consumed by *Bacteroidetes*, *Actinobacteria*, and *Proteobacteria* phylotypes. Canonical cellulose degrading bacteria like *Celvibrio* and members of cosmopolitan yet functionally uncharacterized soil phylogenetic groups like *Chloroflexi*, *Planctomycetes* and *Verrucomicrobia*, specifically the *Spartobacteria*, decomposed cellulose. Cellulose C incorporation into microbial biomass peaked at day 14 and extended through day 30.

**Ecological strategies of soil microorganisms participating in the decomposition of organic matter.** Models of soil C cycling rely on functional niches defined by ecologists and ecological strategies such as growth rate and substrate specificity are parameters for functional niche behavior in soil C models [20]. Functional niches are commonly discovered by observing how community structure changes with changing conditions [21]. In this experiment, DNA-SIP revealed functional niche membership. We also used DNA-SIP data to quantify substrate

specificity which is related to the magnitude of DNA BD shift upon  $^{13}\text{C}$  labeling (see Results). Moreover, we assessed growth rate of functional niche members by estimating niche member *rrn* gene copy number, a genomic feature reliably extrapolated from phylogeny that is indicative of how fast a microorganism grows [17, 22]. We found that  $^{13}\text{C}$ -cellulose responsive OTUs are slow growing substrate specialists relative to  $^{13}\text{C}$ -xylose responders (Figure 4, Figure S8). We also found that  $^{13}\text{C}$ -xylose responsive OTUs that incorporated  $^{13}\text{C}$  into biomass at day one grow faster than OTUs that responded later (Figure 4, Figure S8). If OTUs that first responded after day 1 consumed labeled OTUs that responded at day 1, this suggests that predators and/or saprophytes grow slower than microorganisms directly assimilating labile C and has implications for modelling trophic niches. We also note that  $^{13}\text{C}$ -cellulose responders are generally lower abundance members of the bulk community than  $^{13}\text{C}$ -xylose responsive OTUs (Figure 4), however, High *rrn* gene copy number may inflate  $^{13}\text{C}$ -xylose-responder abundance.

NRI values quantify phylogenetic clustering [23] and have been used to assess clustering of soil OTUs that responded similarly to soil wet up [19, 24]. To our knowledge, assessing phylogenetic clustering of OTUs found to incorporate heavy isotopes into biomass during SIP incubations has not been attempted. We found that  $^{13}\text{C}$ -cellulose and xylose responders are clustered and overdispersed, respectively. This suggests that the ability to degrade cellulose is phylogenetically conserved possibly reflecting the complexity of cellulose degradation biochemistry. The positive relationship between a physiological trait's phylogenetic depth and its complexity has been noted previously [25] and the clade depth of  $^{13}\text{C}$ -cellulose responders, 0.028 16S rRNA gene sequence dissimilarity, is on the same order as that observed for glycoside hydrolases which are diagnostic enzymes for cellulose degradation [26]. Overdispersion, as we saw for the  $^{13}\text{C}$ -xylose responsive OTUs, may be indicative of a readily horizontally transferred trait and/or a trait that is broadly distributed phylogenetically, or, in this case may indicate that the overdispersed group includes more than one trait. It's not clear which  $^{13}\text{C}$ -xylose responsive organisms were labeled as a result of primary xylose assimilation (see below), and therefore it's not clear if  $^{13}\text{C}$ -xylose responsive OTUs in this experiment constitute a single ecologically meaningful group or multiple ecological groups. Temporally defined  $^{13}\text{C}$ -xylose responder groups, however, are phylogenetically coherent (Figure S10, Figure 3). For example, most day 1  $^{13}\text{C}$ -xylose responders are members of the *Paenibacillus* (see Supple-

tal Note XX). Notably, *Paenibacillus* have been previously implicated as labile C decomposers [27].

Intuitively we infer C cycling functional guild diversity from the distribution of diagnostic genes across genomes [26] or from screening culture collections for a particular trait [18]. For instance, the wide distribution of the glycolysis operon in microbial genomes is interpreted as evidence that many soil microorganisms participate in glucose turnover [28]. *In situ* functional guild diversity, however, can vary significantly from diversity assessed by functionally screening isolates and/or genomes. Xylose use in soil, for instance, may be less a function of catabolic pathway distribution across genomes and more a function of lifestyle. Phenomena such as seasonal change [29], and rainfall [24] pulse deliver nutrients and resources to soil. Therefore, fast growth and/or rapid resuscitation upon wet up [24] allow microorganisms to favorably compete for labile C resources. Life history ecological strategies tied to phylogeny like growth rate [21] may constrain the diversity of labile C assimilators even though the ability to use labile C is phylogenetically dispersed. DNA-SIP is useful for establishing *in situ* phylogenetic clustering and diversity of functional guilds because DNA-SIP can account for life history strategies by targeting *active* microorganisms. Additionally, snapshot estimates of community composition commonly inform soil structure-function relationship studies [21] but labile C decomposition might not be linked to snapshot community structure. Alternatively labile C decomposition might be linked specifically to community structure *dynamics*. That is, fast growing spore formers would not need to maintain high abundance to significantly mediate cycling of pulse delivered resources. This accentuates the importance of DNA-SIP for describing soil ecology as DNA-SIP assesses activity which can be decoupled from snapshot abundance.

**Implications for soil C cycling models.** Land management, climate, pollution and disturbance can influence soil community composition [28] which in turn influences soil biogeochemical process rates (e.g. [30]). Assessing functional group diversity and establishing identities of functional group members is necessary to predict how biogeochemical process rates will change with community composition [28, 31]. Aggregate biogeochemical processes that are the sum of many subprocesses involve a broad array of taxa and are assumed to be less influenced by community change than narrow processes that involve a single, specific chemical transformation by a smaller suite of microbial participants [28, 31]. Within an aggregate process such as C decomposition, subprocesses can be fur-

ther classified as broad or narrow [28]. In theory, “broad” and “narrow” functional guilds decompose labile and recalcitrant C, respectively [28].  
 420 However, the diversity of active labile C and recalcitrant C decomposers in soil has not been directly quantified. Notably, we found more OTUs responded to <sup>13</sup>C-cellulose, 63, than <sup>13</sup>C-xylose, 49. Also, it is possible that many <sup>13</sup>C-xylose responders are predatory bacteria or saprophytes as opposed to primary labile C degraders (see below). Cellulose and xylose decomposer functional guilds were non-overlapping in membership – of 104 <sup>13</sup>C-responders only 8 responded to both cellulose and 425 xylose – and represented a small fraction of total soil community diversity (Figure 5). While xylose use is undoubtedly more widely distributed among microbial genomes than the ability to degrade cellulose, the number of unique active cellulose decomposer OTUs outnumbered the number 430 of unique active xylose utilizer OTUs.

Trophic interactions and/or functional groups tuned to different resource concentrations caused the activity succession from *Firmicutes* to *Bacteroidetes* and finally *Actinobacteria* in response to xylose addition. *Actinobacteria* (e.g. *Agromyces*) and *Bacteroidetes* have been previously implicated as predatory soil bacteria [32, 33], and, in our microcosms *Bacteroidetes* and *Actinobacteria* activity peaked while *Firmicutes* <sup>13</sup>C-xylose responder relative abundance plummeted (Figure 2, Figure 3, Figure S6). Considering *Agromyces* and *Bacteroidetes* phylotypes are likely soil predators, one parsimonious hypothesis for <sup>13</sup>C-labelling of *Bacteroidetes* and *Actinobacteria* with a corresponding decrease <sup>13</sup>C-labeled *Firmicutes* abundance is that *Bacteroidetes* and *Actinobacteria* fed on <sup>13</sup>C-labeled *Firmicutes*. Besides predation, mother cell lysis, the last step in sporulation, would release 455 C from spore formers potentially to *Bacteroidetes* and *Actinobacteria*. If the temporal dynamics of <sup>13</sup>C-xylose incorporation are due to trophic interactions, predatory bacteria or saprophytes consumed many, if not most, fast-growing labile C degraders. Hence, soil C cycling models should include trophic interactions between soil bacteria but rarely do (e.g. [34]). When soil C models do account for predators/saprophytes, trophic interactions are predicted to significantly influence C:N ratios of SOM relative to litter C:N, and, recycle significant amounts of microbial biomass [20].

We propose two scenarios in the context of our results whereby community composition could affect C dynamics and fate. Genomic evidence shows 470 cellulose degradation is a phylogenetically conserved trait [26]. Our study evaluates the phylogenetic conservation of soil cellulose degradation in active microorganisms via DNA-SIP and genomic evidence concurs with our results. A de-

crease in cellulose degrader abundance would diminish cellulose decomposition process rates as few soil microorganisms can fill the phylogenetically conserved cellulose degradation niche. Dispersed cellulose decomposers could renew ecosystem function, however. For labile C decomposition, the absence of fast growing spore formers would allow other microbes to assimilate labile C provided dispersal does not enable rapid recolonization. Primary labile C degraders in this study grow fast, and form spores and these distinct ecological strategies might indicate distinct C use dynamics and/or resource allocation. New labile C degraders may metabolize and allocate labile C differently thus changing labile C dynamics and fate. Further, labile C degrader substitution could affect biomass C turnover by predatory bacteria or saprophytes that feed on fast growing, spore forming labile C decomposers. On the other hand, spore formation enables dispersal [35] which would allow fast growing spore formers to continuously occupy the labile C decomposition niche. One proposed mechanism for similar decomposition rates of labile C across soils varying in community composition is that labile C is decomposed by a diverse suite of soil microorganisms [28]. An alternative hypothesis for consistent labile C process rates across different soils is that labile C degraders disperse readily. Notably, other lineages implicated in rapid labile C turnover include members of the *Actinobacteria* [24] and many soil *Actinobacteria* form hyphae that facilitate dispersal [36]. The two hypotheses are not mutually exclusive, but our results and previous studies suggest that environmental conditions unfavorable to fast-growing spore-formers and/or quickly resuscitated, hyphal *Actinobacteria* may impact labile C dynamics and fate.

**Conclusion.** Microorganisms sequester atmospheric C and respire SOM influencing climate change on a global scale but we do not know which microorganisms carry out specific soil C transformations. In this experiment microbes from physiologically uncharacterized but ubiquitous soil lineages participated in cellulose decomposition. Cellulose C degraders included members of the *Verrucomicrobia* (*Spartobacteria*), *Chloroflexi*, *Bacteroidetes* and *Planctomycetes*. *Spartobacteria* in particular are globally cosmopolitan soil microorganisms and are often the most abundant *Verrucomicrobia* order in soil [37]. Fast-growing *Firmicutes* spore formers assimilated labile C in our microcosms. *Bacteroidetes* and *Actinobacteria* phylotypes, previously implicated as predators, may have fed on the fast growing *Firmicutes*. Our results suggest that, cosmopolitan *Spartobacteria* may degrade cellulose on a global scale, bacterial trophic interactions can

significantly impact soil C cycling, and life history ecological strategies such as fast growth constrain functional guild diversity for labile C decomposi-  
590 tion.

## Methods

Additional information on sample collection and analytical methods is provided in Supplemental Materials and Methods.

540 Twelve soil cores (5 cm diameter x 10 cm depth) were collected from six random sampling locations within an organically managed agricultural field in Penn Yan, New York. Soils were pretreated by sieving (2 mm), homogenizing sieved soil, and pre-  
545 incubating 10 g of dry soil weight in flasks for 2 weeks. Soils were amended with a 5.3 mg g soil<sup>-1</sup> carbon mixture; representative of natural concentrations [38]. Mixture contained 38% cellulose, 23% lignin, 20% xylose, 3% arabinose, 1% galac-  
550 tose, 1% glucose, and 0.5% mannose by mass, with the remaining 13.5% mass composed of an amino acid (in-house made replica of Teknova C0705) and basal salt mixture (Murashige and Skoog, Sigma Aldrich M5524). Three parallel treatments were  
555 performed; (1) unlabeled control, (2)<sup>13</sup>C-cellulose, (3)<sup>13</sup>C-xylose (98 atom% <sup>13</sup>C, Sigma Aldrich). Each treatment had 2 replicates per time point (n = 4) except day 30 which had 4 replicates; total microcosms per treatment n = 12, except <sup>13</sup>C-  
560 cellulose which was not sampled at day 1, n = 10. Other details relating to substrate addition can be found in SI. Microcosms were sampled de-  
structively (stored at -80°C until nucleic acid pro-  
cessing) at days 1 (control and xylose only), 3, 7,  
565 14, and 30.

Nucleic acids were extracted using a modified Griffiths protocol [39]. To prepare nucleic acid extracts for isopycnic centrifugation as previously described [40], DNA was size selected (>4kb) using  
570 1% low melt agarose gel and β-agarase I enzyme extraction per manufacturers protocol (New England Biolab, M0392S). For each time point in the series isopycnic gradients were setup using a modified protocol [41] for a total of five <sup>12</sup>C-control, five  
575 <sup>13</sup>C-xylose, and four <sup>13</sup>C-cellulose microcosms. A density gradient (average density 1.69 g mL<sup>-1</sup>) solution of 1.762 g cesium chloride (CsCl) ml<sup>-1</sup> in gradient buffer solution (pH 8.0 15 mM Tris-HCl, 15 mM EDTA, 15 mM KCl) was used to sepa-  
580 rate <sup>13</sup>C-enriched and <sup>12</sup>C-nonenriched DNA. Each gradient was loaded with approximately 5 µg of DNA and ultracentrifuged for 66 h at 55,000 rpm and room temperature (RT). Fractions of ~100 µL were collected from below by displacing the DNA-  
585 CsCl-gradient buffer solution in the centrifugation tube with water using a syringe pump at a flow rate of 3.3 µL s<sup>-1</sup> [42] into Acroprep<sup>TM</sup> 96 filter

plate (Pall Life Sciences 5035). The refractive index of each fraction was measured using a Reichert AR200 digital refractometer modified as previously described [40] to measure a volume of 5 µL. Then buoyant density was calculated from the refractive index as previously described [40] (see also SI). The collected DNA fractions were purified by repetitive washing of Acroprep filter wells with TE. Finally, 50 µL TE was added to each fraction then resuspended DNA was pipetted off the filter into a new microfuge tube.

For every gradient, 20 fractions were chosen for sequencing between the density range 1.67–1.75 g mL<sup>-1</sup>. Barcoded 454 primers were designed using 454-specific adapter B, 10 bp barcodes [43], a 2 bp linker (5'-CA-3'), and 806R primer for reverse primer (BA806R); and 454-specific adapter A, a 2 bp linker (5'-TC-3'), and 515F primer for forward primer (BA515F). Each fraction was PCR amplified using 0.25 µL 5 U µl<sup>-1</sup> AmpliTaq Gold (Life Technologies, Grand Island, NY; N8080243), 2.5 µL 10X Buffer II (100 mM Tris-HCl, pH 8.3, 500 mM KCl), 2.5 µL 25 mM MgCl<sub>2</sub>, 4 µL 5 mM dNTP, 1.25 µL 10 mg mL<sup>-1</sup> BSA, 0.5 µL 10 µM BA515F, 1 µL 5 µM BA806R, 3 µL H<sub>2</sub>O, 10 µL 1:30 DNA template) in triplicate. Samples were normalized either using Pico green quantification and manual calculation or by SequalPrep<sup>TM</sup> normalization plates (Invitrogen, Carlsbad, CA; A10510), then pooled in equimolar concentrations. Pooled DNA was gel extracted from a 1% agarose gel using Wizard SV gel and PCR clean-up system (Promega, Madison, WI; A9281) per manufacturer's protocol. Amplicons were sequenced on Roche 454 FLX system using titanium chemistry at Selah Genomics (formerly EnGenCore, Columbia, SC)

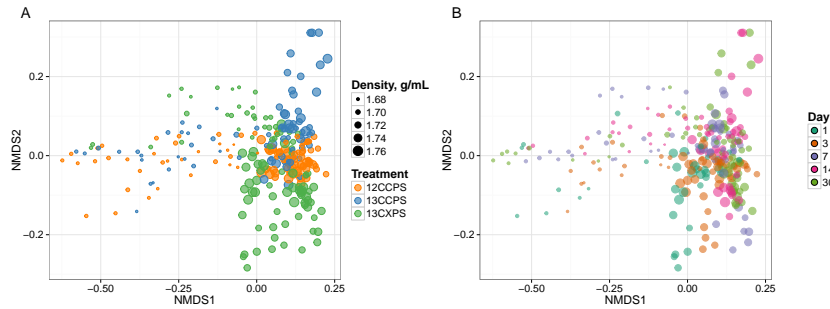
## References

- Amundson R (2001) The carbon budget in soils. *Annu Rev Earth Planet Sci* 29(1): 535–562.
- Batjes N-H (1996) Total carbon and nitrogen in the soils of the world. *European Journal of Soil Science* 47(2): 151–163.
- Chapin F (2002) Principles of terrestrial ecosystem ecology.
- Groenigen K-J, Graaff M-A, Six J, Harris D, Kuikman P, Kessel C (2006) The impact of elevated atmospheric CO<sub>2</sub> on soil C and N dynamics: a meta-analysis. *Managed Ecosystems and CO<sub>2</sub>* (Springer Science, Berlin Heidelberg), pp 373–391.
- Friedlingstein P, Cox P, Betts R, Bopp L, von W-B, Brovkin V, et al. (2006) Climate–carbon cycle feedback analysis: Results from the C4 model intercomparison. *J Climate* 19(14):

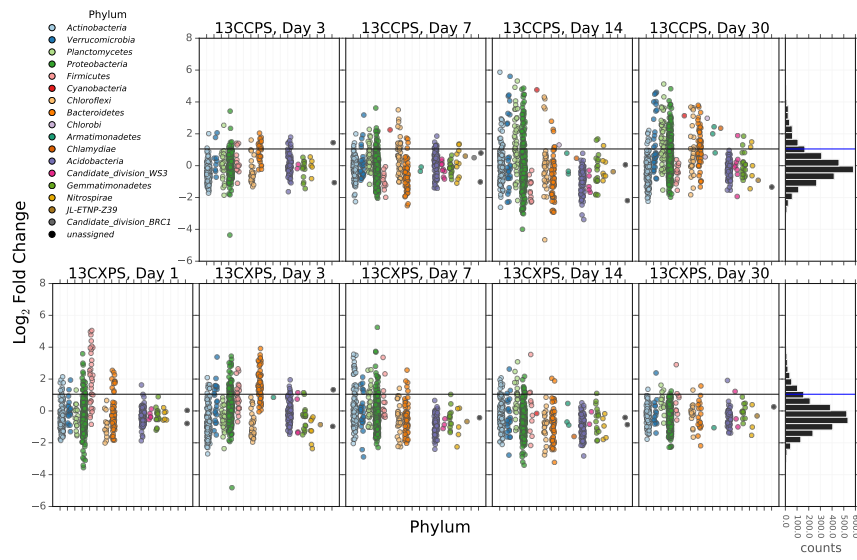
- 3337–3353.
6. Neff J-C, Asner G-P (2001) Dissolved organic carbon in terrestrial ecosystems: synthesis and a model. *Ecosystems* 4(1): 29–48.
7. *Warning: citation key “McGuire2010a” is not in the bibliography database.*
8. O’Donnell A-G, Seasman M, Macrae A, Waite I, Davies J-T (2002) Plants and fertilisers as drivers of change in microbial community structure and function in soils. *Interactions in the Root Environment: An Integrated Approach* (Springer, Netherlands), pp 135–145.
9. Coleman D-C, Crossley D-A (1996) Fundamentals of Soil Ecology.
10. Nannipieri P, Ascher J, Ceccherini M-T, Landi L, Pietramellara G, Renella G (2003) Microbial diversity and soil functions. *European Journal of Soil Science* 54(4): 655–670.
11. Chen Y, Murrell J-C (2010) When metagenomics meets stable-isotope probing: progress and perspectives. *Trends Microbiol* 18(4): 157–163.
12. Lu Y (2005) In situ stable isotope probing of methanogenic archaea in the rice rhizosphere. *Science* 309(5737): 1088–1090.
13. Anderson M-J (2001) A new method for non-parametric multivariate analysis of variance. *Austral Ecology* 26(1): 32–46.
14. Anderson M-J, Ellingsen K-E, McArdle B-H (2006) Multivariate dispersion as a measure of beta diversity. *Ecology Letters* 9(6): 683–693.
15. Oksanen J, Kindt R, Legendre P, OHara B, Stevens M-HH, Oksanen M-J, et al. (2007) The vegan package.
16. Benjamini Y, Hochberg Y (1995) Controlling the false discovery rate: a practical and powerful approach to multiple testing. *Journal of the Royal Statistical Society, Series B* 57(1): 289–300.
17. Kembel S-W, Wu M, Eisen J-A, Green J-L (2012) Incorporating 16S gene copy number information improves estimates of microbial diversity and abundance. *PLoS Comput Biol* 8(10): e1002743.
18. Martiny A-C, Treseder K, Pusch G (2013) Phylogenetic conservatism of functional traits in microorganisms. *ISMEJ* 7(4): 830–838.
19. Evans S-E, Wallenstein M-D (2014) Climate change alters ecological strategies of soil bacteria. *Ecol Lett* 17(2): 155–164.
20. Kaiser C, Franklin O, Dieckmann U, Richter A (2014) Microbial community dynamics alleviate stoichiometric constraints during litter decay. *Ecol Lett* 17(6): 680–690.
21. Fierer N, Bradford M-A, Jackson R-B (2007) Toward an ecological classification of soil bacteria. *Ecology* 88(6): 1354–1364.
22. Klappenbach J, Saxman P, Cole J, Schmidt T (2001) rrndb: the Ribosomal RNA Operon Copy Number Database.. *Nucleic Acids Res* 29(1): 181–184.
23. Webb C-O (2000) Exploring the phylogenetic structure of ecological communities: an example for rain forest trees.. *The American Naturalist* 156(2): 145–155.
24. Placella S-A, Brodie E-L, Firestone M-K (2012) Rainfall-induced carbon dioxide pulses result from sequential resuscitation of phylogenetically clustered microbial groups. *PNAS* 109(27): 10931–10936.
25. Martiny A-C, Treseder K, Pusch G (2013) Phylogenetic conservatism of functional traits in microorganisms. *ISMEJ* 7(4): 830–838.
26. Berlemont R, Martiny A-C (2013) Phylogenetic distribution of potential cellulases in bacteria. *Appl Environ Microbiol* 79(5): 1545–1554.
27. Verastegui Y, Cheng J, Engel K, Kolczynski D, Mortimer S, Lavigne J, et al. (2014) Multisubstrate isotope labeling and metagenomic analysis of active soil bacterial communities. *mBio* 5(4): e01157–14.
28. McGuire K-L, Treseder K-K (2010) Microbial communities and their relevance for ecosystem models: Decomposition as a case study. *Soil Biology and Biochemistry* 42(4): 529–535.
29. Schmidt S-K, Costello E-K, Nemergut D-R, Cleveland C-C, Reed S-C, Weintraub M-N, et al. (2007) Biogeochemical consequences of rapid microbial turnover and seasonal succession in soil. *Ecology* 88(6): 1379–1385.
30. Berlemont R, Allison S-D, Weihe C, Lu Y, Brodie E-L, Martiny J-BH, et al. (2014) Cellulolytic potential under environmental changes in microbial communities from grassland litter. *Front Microbiol* 5: 639.
31. Schimel J (1995) Ecosystem consequences of microbial diversity and community structure. *Arctic and alpine biodiversity: patterns, causes and ecosystem consequences*, , eds. III P-DFSC, Körner P-DC, Ecological Studies (Springer, Berlin Heidelberg), pp 239–254.
32. Lueders T, Kindler R, Miltner A, Friedrich M-W, Kaestner M (2006) Identification of bacterial micropredators distinctively active in a soil microbial food web. *Appl Environ Microbiol* 72(8): 5342–5348.
33. Casida L-E (1983) Interaction of Agromyces ramosus with Other Bacteria in Soil.. *Appl Environ Microbiol* 46(4): 881–888.
34. Moore J-C, Walter D-E, Hunt H-W (1988) Arthropod Regulation of Micro- and Mesobiota in Below-Ground Detrital Food Webs. *Annu Rev Entomol* 33(1): 419–435.



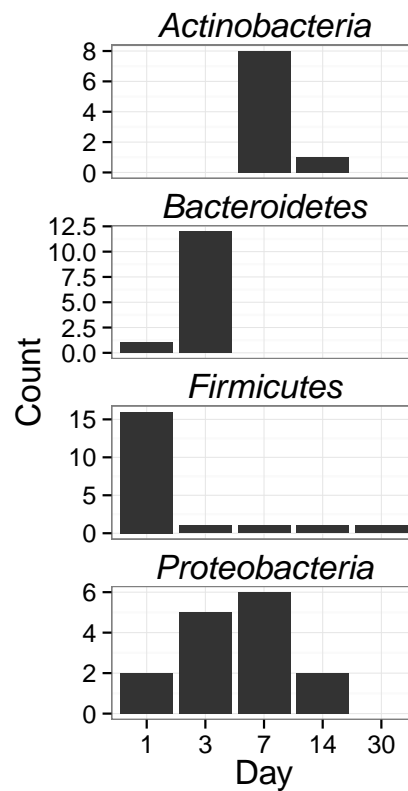
- 760 35. Nicholson W-L, Munakata N, Horneck G,  
Melosh H-J, Setlow P (2000) Resistance of  
bacillus endospores to extreme terrestrial and  
extraterrestrial environments. *Microbiol Mol  
Biol Rev* 64(3): 548–572.
- 765 36. Killham K, Prosser J-I (2007) The prokary-  
otes. *Soil Microbiology, Ecology and Biochem-  
istry (Third Edition)*, , ed. PAUL E-A (Aca-  
demic Press, San Diego), pp 119–144.
- 770 37. Bergmann G-T, Bates S-T, Eilers K-G, Lauber C-L, Caporaso J-G, Walters W-A, et al. (2011)  
The under-recognized dominance of Verru-  
comicrobia in soil bacterial communities. *Soil  
Biology and Biochemistry* 43(7): 1450–1455.
- 775 38. Schneckenberger K, Demin D, Stahr K, Kuzyakov Y (2008) Microbial utilization and  
mineralization of  $^{14}\text{C}$  glucose added in six or-  
ders of concentration to soil. *Soil Biology and  
Biochemistry* 40(8): 1981–1988.
- 780 39. Griffiths R-I, Whiteley A-S, O'Donnell A-G, Bailey M-J (2000) Rapid method for coex-  
traction of DNA and RNA from natural en-  
vironments for analysis of ribosomal DNA—  
and rRNA-based microbial community compo-  
sition. *Appl Environ Microbiol* 66(12): 5488–  
5491.
- 785 40. Buckley D-H, Huangyutitham V, Hsu S-F,  
Nelson T-A (2007) Stable isotope probing  
with  $^{15}\text{N}$  achieved by disentangling the effects  
of genome G+C content and isotope enrich-  
ment on dna Density. *Appl Environ Microbiol*  
73(10): 3189–3195.
41. Neufeld J-D, Vohra J, Dumont M-G, Lueders T, Manefield M, Friedrich M-W, et al. (2007)  
DNA stable-isotope probing. *Nature Protocols*  
2(4): 860–866.
42. Manefield M, Whiteley A-S, Griffiths R-I, Bai-  
ley M-J (2002) RNA Stable isotope probing a  
novel means of linking microbial community  
function to phylogeny. *Appl Environ Microbiol*  
68(11): 5367–5373.
43. Hamady M, Walker J-J, Harris J-K, Gold N-  
J, Knight R (2008) Error-correcting barcoded  
primers for pyrosequencing hundreds of sam-  
ples in multiplex. *Nat Meth* 5(3): 235–237.



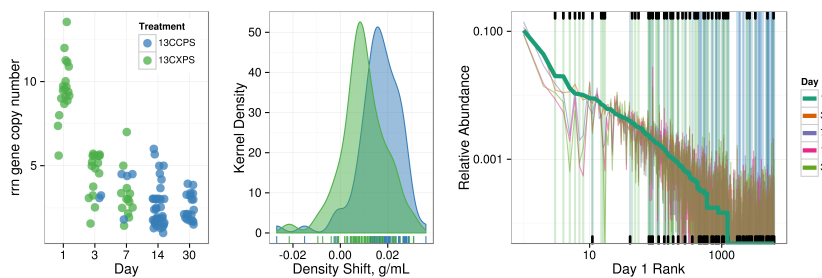
**Fig. 1.** NMDS analysis from weighted unifrac distances of 454 sequence data from SIP fractions of each treatment over time. Twenty fractions from a CsCl gradient fractionation for each treatment at each time point were sequenced (Fig. S1). Each point on the NMDS represents the bacterial composition based on 16S sequencing for a single fraction where the size of the point is representative of the density of that fraction and the colors represent the treatments (A) or days (B).



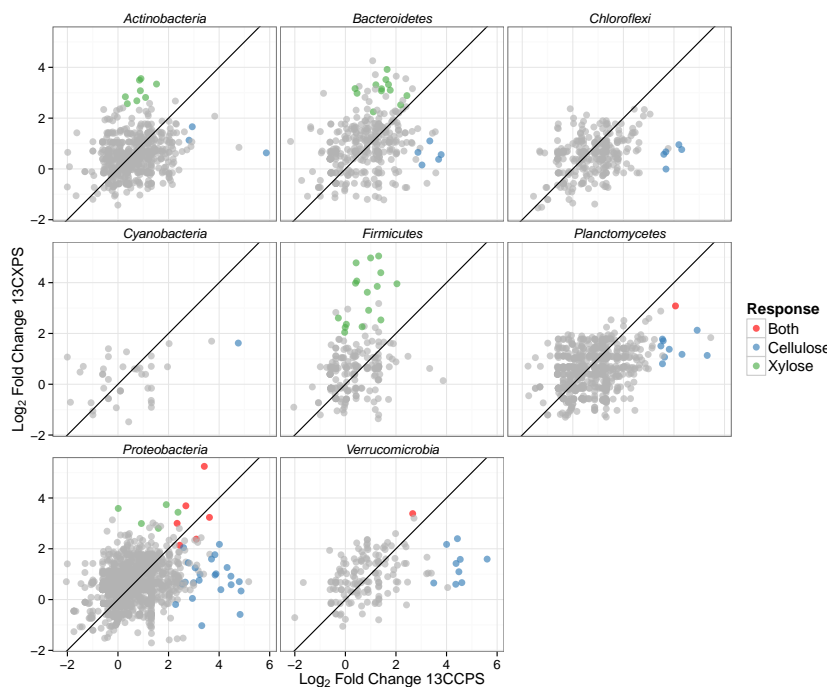
**Fig. 2.** Log<sub>2</sub> fold change of <sup>13</sup>C-responders in cellulose treatment (top) and xylose treatment (bottom). Log<sub>2</sub> fold change is based on the relative abundance in the experimental treatment compared to the control within the density range 1.7125–1.755 g ml<sup>-1</sup>. Taxa are colored by phylum. ‘Counts’ is a histogram of log<sub>2</sub> fold change values.



**Fig. 3.** Counts of  $^{13}\text{C}$ -xylose responders in the *Actinobacteria*, *Bacteroidetes*, *Firmicutes* and *Proteobacteria* at days 1, 3, 7 and 30.

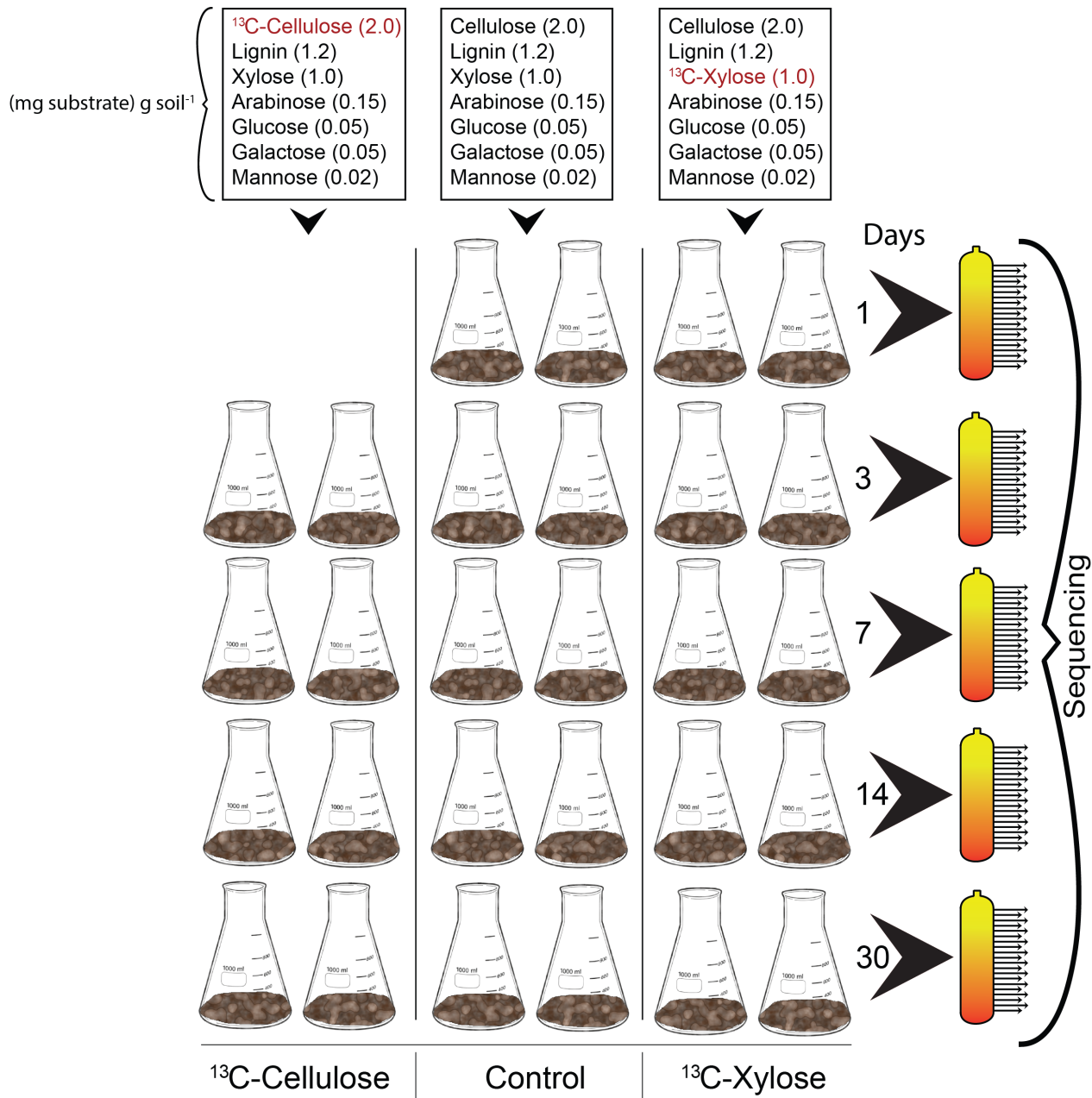


**Fig. 4.**  $^{13}\text{C}$ -responder characteristics based on density shift (A) and rank (B). Kernel density estimation of  $^{13}\text{C}$ -responder's density shift in cellulose treatment (blue) and xylose treatment (green) demonstrates degree of labeling for responders for each respective substrate.  $^{13}\text{C}$ -responders in rank abundance are labeled by substrate (cellulose, blue; xylose, green). Ticks at top indicate location of  $^{13}\text{C}$ -xylose responders in bulk community. Ticks at bottom indicate location of  $^{13}\text{C}$ -cellulose responders in bulk community. OTU rank was assessed from day 1 bulk samples.

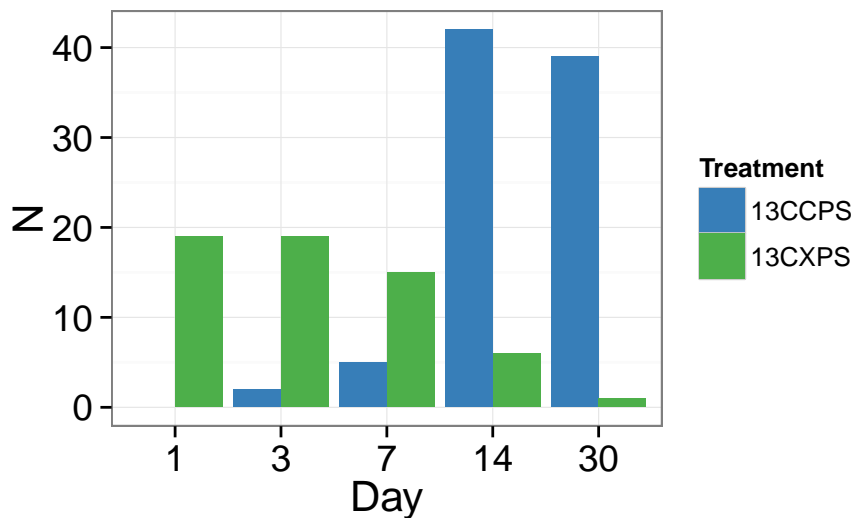


**Fig. 5.** Maximum log<sub>2</sub> fold change in response to labeled substrate incorporation for each substrate and all OTUs that pass sparsity filtering in both substrate analyses. Points colored by response. Line has slope of 1 with intercept at the origin. OTUs falling in the top-right quadrant responded to both substrates while those in the top-left and bottom-right responded to <sup>13</sup>C-xylose and <sup>13</sup>C-cellulose, respectively.

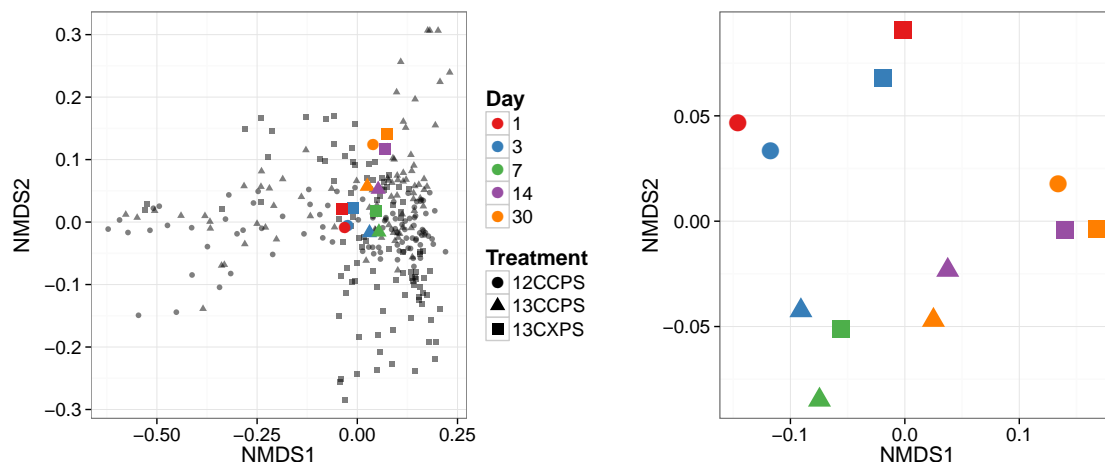
**Supplemental Figures and Tables**



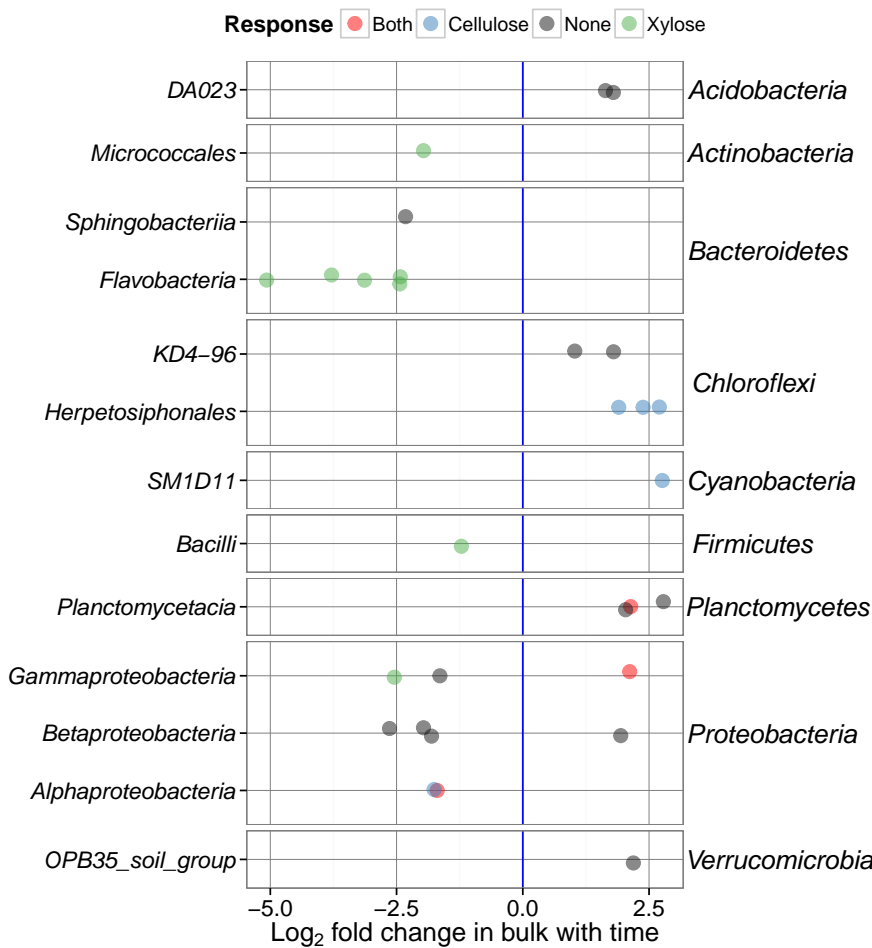
**Fig. S1.** The experimental design. A carbon mixture, in addition to inorganic salts and amino acids (not shown here), was added to each soil microcosm where the only difference between treatments is the <sup>13</sup>C-labeled isotope (in red). At days 1, 3, 7, 14, and 30 replicate microcosms were destructively harvested for downstream molecular applications. Bulk DNA from each treatment and time point ( $n = 14$ ) was CsCl density separated by centrifuged and fractionated (orange tubes wherein each arrow represents a fraction from the density gradient). Fractions were 16S gene sequenced using next generation sequencing technology.



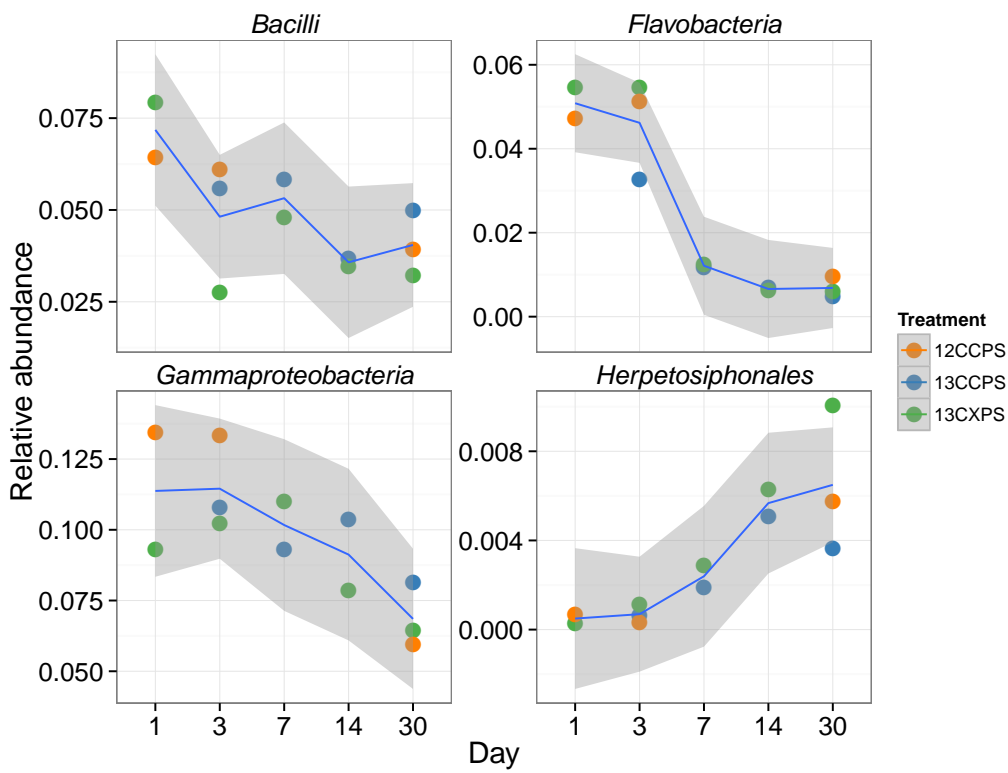
**Fig. S2.** Counts of responders to each isotopically labeled substrate (cellulose and xylose) over time.



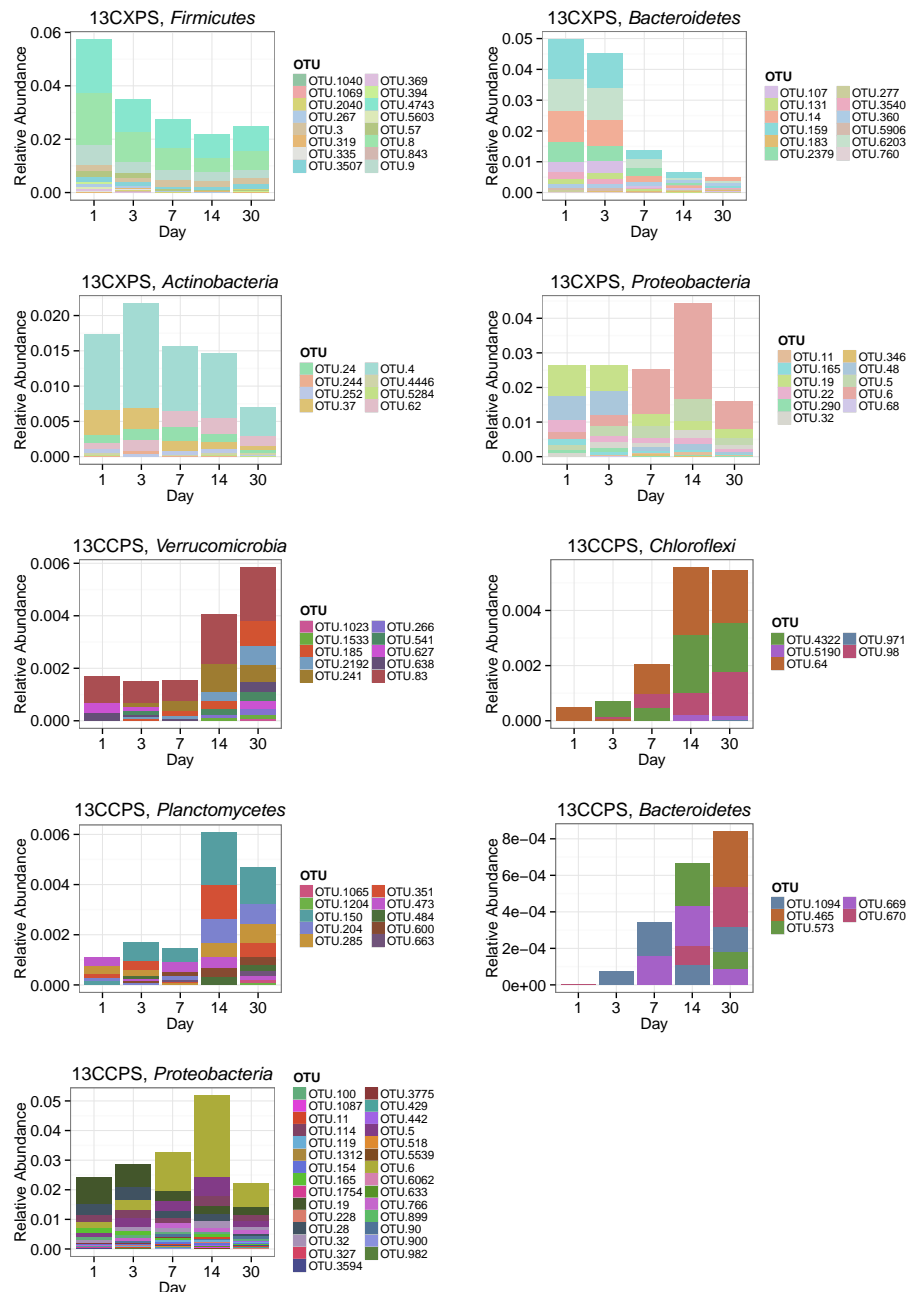
**Fig. S3.** Ordination of bulk gradient fraction phylogenetic profiles.



**Fig. S4.** Fold change time<sup>-1</sup> for OTUs that changed significantly in abundance over time. One panel per phylum (phyla indicated on the right). Taxonomic class indicated on the left.



**Fig. S5.** Relative abundance versus day for classes that changed significantly in relative abundance with time.

**Fig. S6.** Sum of bulk abundances with selected phylum for responder OTUs.

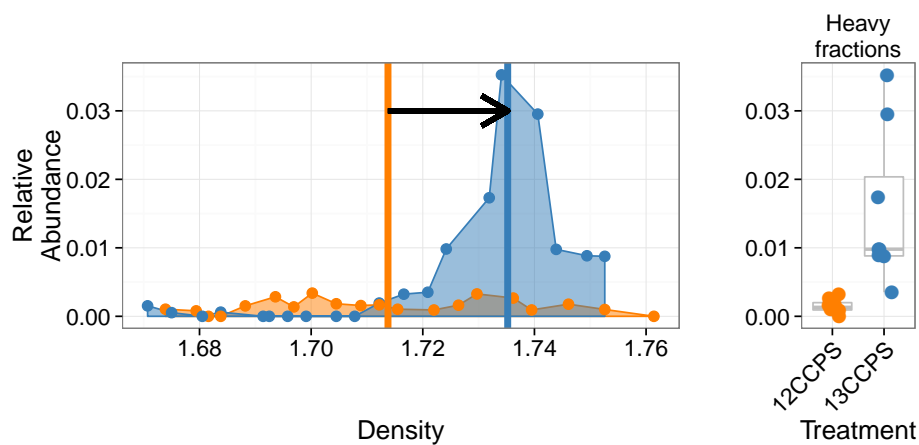


**Fig. S7.** Density profile for a single  $^{13}\text{C}$ -cellulose “responder” OTU in the labeled gradient, blue, and the control gradient, orange. Vertical lines show center of mass for each density profile and arrow denotes the magnitude and direction of the BD shift upon labeling. Panel at right shows relative abundance values in the heavy fractions for each gradient.

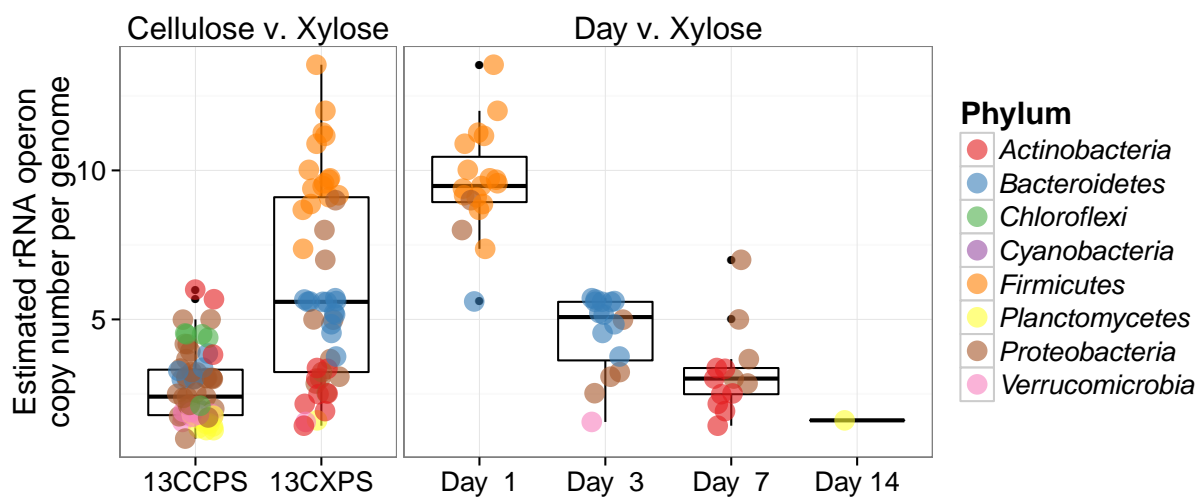


**Fig. S8.** Estimated rRNA operon copy number per genome for  $^{13}\text{C}$  responding OTUs. Panel titles indicate which labeled substrate(s) are depicted.

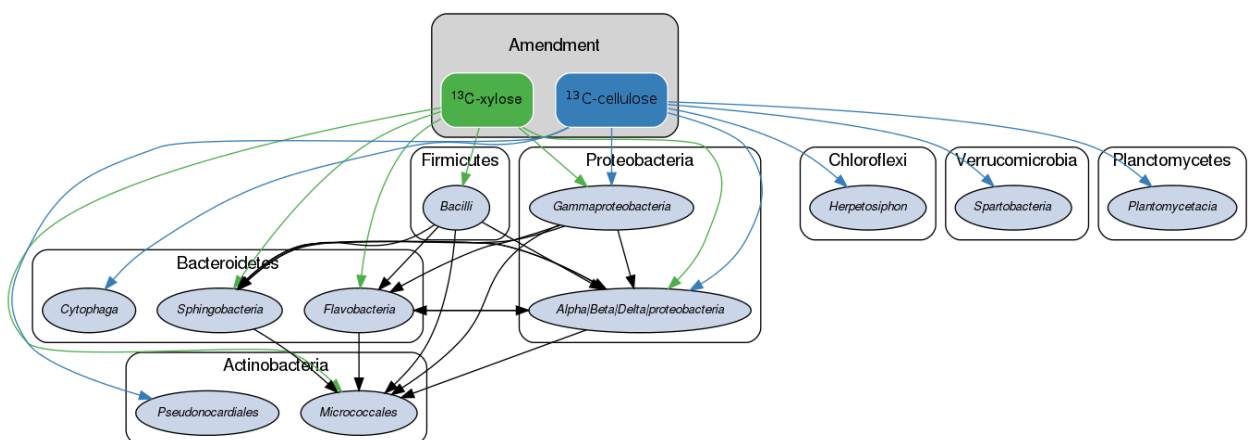


**Fig. S9.** Conceptual model of soil food web in this experiment. Taxa shown possessed at least two <sup>13</sup>C responder OTUs for a given C substrate. *Proteobacteria* response was too varied taxonomically to depict at higher taxonomic resolution in this format. Black arrows indicate possible predator/prey interactions whereas colored arrows represent possible routes of primary degradation (green: xylose, blue: cellulose).

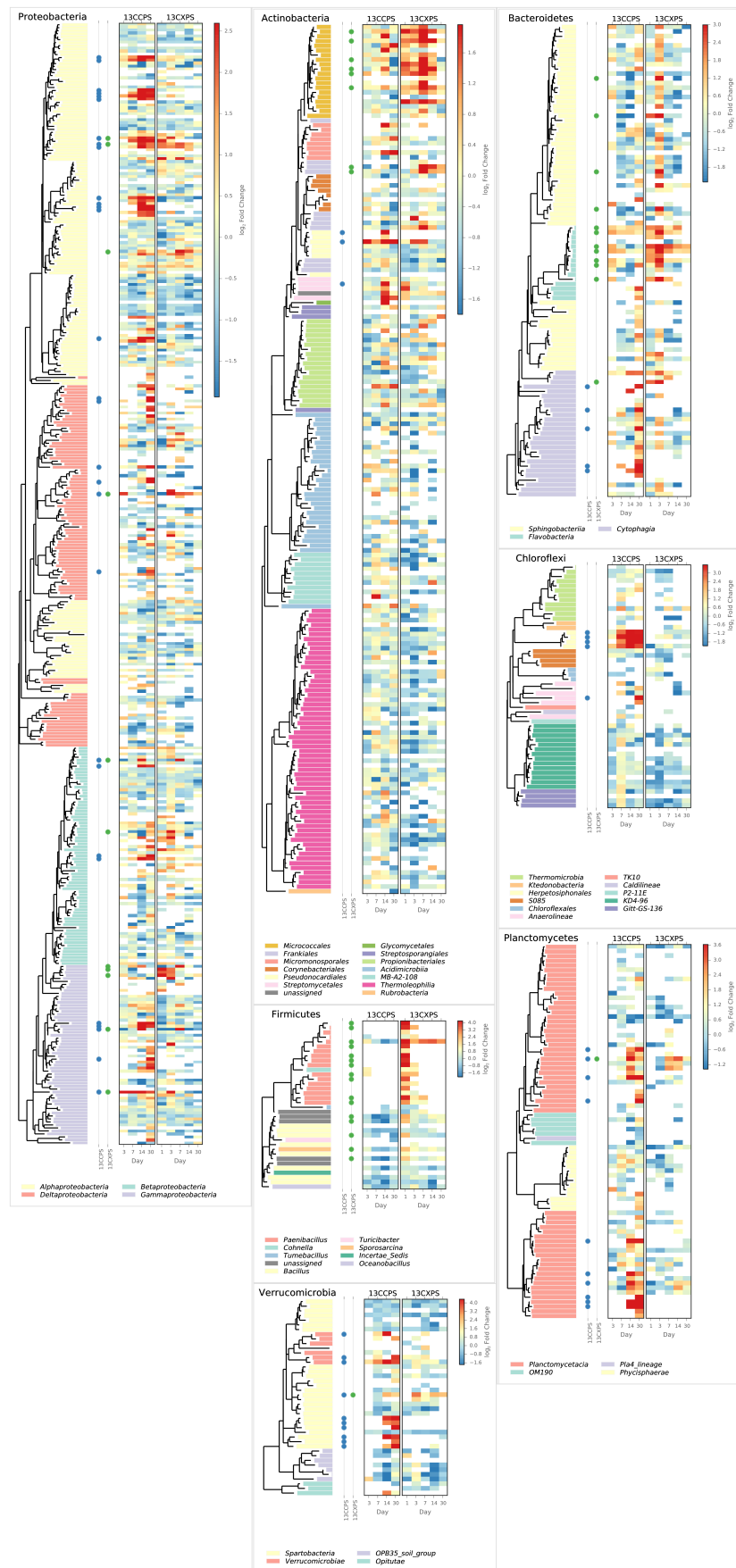


**Fig. S10.** Phylum specific trees. Heatmap indicates fold change between heavy fractions of control gradients versus labeled gradients. Dots indicate the position of “responders” to  $^{13}\text{C}$ -xylose (green) or  $^{13}\text{C}$ -cellulose (blue).

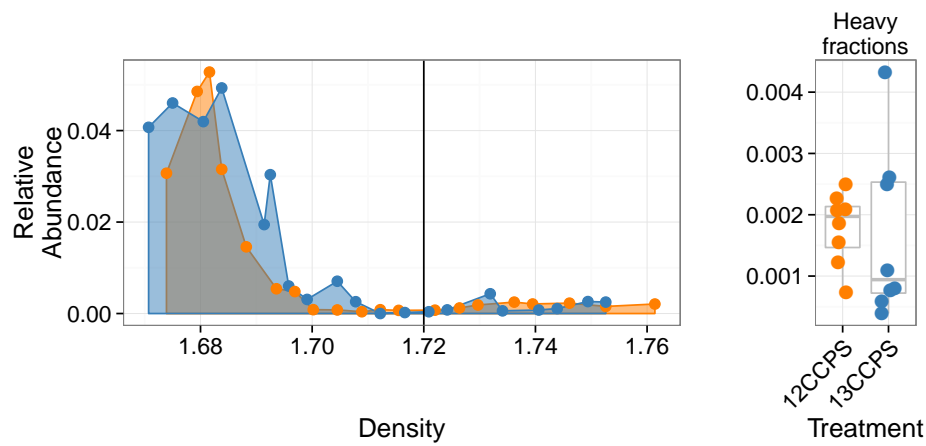


**Fig. S11.** Density profile for a single  $^{13}\text{C}$ -cellulose "non-responder" OTU in the labeled gradient, blue, and the control gradient, orange. Vertical line shows where "heavy" fractions begin as defined in our analysis. Panel at right shows relative abundance values in the heavy fractions for each gradient.

Table S1: <sup>13</sup>C-cellulose responders BLAST against Living Tree Project

OTU ID	Fold change <sup>a</sup>	Day <sup>b</sup>	Top BLAST hits	BLAST %ID	Phylum;Class;Order
OTU.100	2.66	14	<i>Pseudoxanthomonas sacheonensis</i> , <i>Pseudoxanthomonas dokdonensis</i>	100.0	Proteobacteria Gammaproteobacteria Xanthomonadales
OTU.1023	4.61	30	No hits of at least 90% identity	80.54	Verrucomicrobia Spartobacteria Chthoniobacterales
OTU.1065	5.31	14	No hits of at least 90% identity	84.55	Planctomycetes Planctomycetacia Planctomycetales
OTU.1087	4.32	14	<i>Devsia soli</i> , <i>Devsia crocina</i> , <i>Devsia riboflavina</i>	99.09	Proteobacteria Alphaproteobacteria Rhizobiales
OTU.1094	3.69	30	<i>Sporocytophaga myxococcoides</i>	99.55	Bacteroidetes Cytophagia Cytophagales
OTU.11	3.41	14	<i>Stenotrophomonas pavanii</i> , <i>Stenotrophomonas maltophilia</i> , <i>Pseudomonas geniculata</i>	99.54	Proteobacteria Gammaproteobacteria Xanthomonadales
OTU.114	2.78	14	<i>Herbaspirillum sp. SUEMI03</i> , <i>Herbaspirillum sp. SUEMI10</i> , <i>Oxalicibacterium solurbis</i> , <i>Herminiumonas fonticola</i> , <i>Oxalicibacterium horti</i>	100.0	Proteobacteria Betaproteobacteria Burkholderiales
OTU.119	3.31	14	<i>Brevundimonas alba</i>	100.0	Proteobacteria Alphaproteobacteria Caulobacterales
OTU.120	4.76	14	<i>Vampirovibrio chlorellavorus</i>	94.52	Cyanobacteria SM1D11 uncultured-bacterium
OTU.1204	4.32	30	<i>Planctomyces limnophilus</i>	91.78	Planctomycetes Planctomycetacia Planctomycetales
OTU.1312	4.07	30	<i>Paucimonas lemoignei</i>	99.54	Proteobacteria Betaproteobacteria Burkholderiales
OTU.132	2.81	14	<i>Streptomyces spp.</i>	100.0	Actinobacteria Streptomycetales Streptomycetaceae
OTU.150	4.06	14	No hits of at least 90% identity	86.76	Planctomycetes Planctomycetacia Planctomycetales
OTU.1533	3.43	30	No hits of at least 90% identity	82.27	Verrucomicrobia Spartobacteria Chthoniobacterales
OTU.154	3.24	14	<i>Pseudoxanthomonas mexicana</i> , <i>Pseudoxanthomonas japonensis</i>	100.0	Proteobacteria Gammaproteobacteria Xanthomonadales
OTU.165	3.1	14	<i>Rhizobium skieniewicense</i> , <i>Rhizobium vignae</i> , <i>Rhizobium larrymoorei</i> , <i>Rhizobium alkalisolii</i> , <i>Rhizobium galegae</i> , <i>Rhizobium huautlense</i>	100.0	Proteobacteria Alphaproteobacteria Rhizobiales
OTU.1754	4.48	14	<i>Asticcacaulis biprosthecium</i> , <i>Asticcacaulis benevestitus</i>	96.8	Proteobacteria Alphaproteobacteria Caulobacterales
OTU.185	4.37	14	No hits of at least 90% identity	85.14	Verrucomicrobia Spartobacteria Chthoniobacterales
OTU.19	2.44	14	<i>Rhizobium alamii</i> , <i>Rhizobium mesosinicum</i> , <i>Rhizobium mongolense</i> , <i>Arthrobacter viscosus</i> , <i>Rhizobium sullae</i> , <i>Rhizobium yanglingense</i> , <i>Rhizobium loessense</i>	99.54	Proteobacteria Alphaproteobacteria Rhizobiales
OTU.204	3.81	14	No hits of at least 90% identity	nan	Planctomycetes Planctomycetacia Planctomycetales

Table S1 – continued from previous page

OTU ID	Fold change	Day	Top BLAST hits	BLAST %ID	Phylum;Class;Order
OTU.2192	3.49	30	No hits of at least 90% identity	83.56	Verrucomicrobia Spartobacteria Chthoniobacterales
OTU.228	2.54	30	<i>Sorangium cellulosum</i>	98.17	Proteobacteria Deltaproteobacteria Myxococcales
OTU.241	2.66	14	No hits of at least 90% identity	87.73	Verrucomicrobia Spartobacteria Chthoniobacterales
OTU.257	2.94	14	<i>Lentzea waywayandensis</i> , <i>Lentzea flaviverrucosa</i>	100.0	Actinobacteria Pseudonocardiales Pseudonocardiaceae
OTU.266	4.54	30	No hits of at least 90% identity	83.64	Verrucomicrobia Spartobacteria Chthoniobacterales
OTU.28	2.59	14	<i>Rhizobium giardinii</i> , <i>Rhizobium tubonense</i> , <i>Rhizobium tibeticum</i> , <i>Rhizobium mesoamericanum CCGE 501</i> , <i>Rhizobium herbae</i> , <i>Rhizobium endophyticum</i>	99.54	Proteobacteria Alphaproteobacteria Rhizobiales
OTU.285	3.55	30	<i>Blastopirellula marina</i>	90.87	Planctomycetes Planctomycetacia Planctomycetales
OTU.32	2.34	3	<i>Sandaracinus amyloyticus</i>	94.98	Proteobacteria Deltaproteobacteria Myxococcales
OTU.327	2.99	14	<i>Asticcacaulis biprosthecum</i> , <i>Asticcacaulis benevestitus</i>	98.63	Proteobacteria Alphaproteobacteria Caulobacterales
OTU.351	3.54	14	<i>Pirellula staleyi DSM 6068</i>	91.86	Planctomycetes Planctomycetacia Planctomycetales
OTU.3594	3.83	30	<i>Chondromyces robustus</i>	90.41	Proteobacteria Deltaproteobacteria Myxococcales
OTU.3775	3.88	14	<i>Devosia glacialis</i> , <i>Devosia chinhatensis</i> , <i>Devosia geojensis</i> , <i>Devosia yakushimensis</i>	98.63	Proteobacteria Alphaproteobacteria Rhizobiales
OTU.429	3.7	30	<i>Devosia limi</i> , <i>Devosia psychrophila</i>	97.72	Proteobacteria Alphaproteobacteria Rhizobiales
OTU.4322	4.19	14	No hits of at least 90% identity	89.14	Chloroflexi Herpetosiphonales Herpetosiphonaceae
OTU.442	3.05	30	<i>Chondromyces robustus</i>	92.24	Proteobacteria Deltaproteobacteria Myxococcales
OTU.465	3.79	30	<i>Ohtaekwangia kribbensis</i>	92.73	Bacteroidetes Cytophagia Cytophagales
OTU.473	3.58	14	<i>Pirellula staleyi DSM 6068</i>	90.91	Planctomycetes Planctomycetacia Planctomycetales
OTU.484	4.92	14	No hits of at least 90% identity	89.09	Planctomycetes Planctomycetacia Planctomycetales
OTU.5	2.69	14	<i>Delftia tsuruhatensis</i> , <i>Delftia lacustris</i>	100.0	Proteobacteria Betaproteobacteria Burkholderiales
OTU.518	4.8	14	<i>Hydrogenophaga intermedia</i>	100.0	Proteobacteria Betaproteobacteria Burkholderiales
OTU.5190	3.6	30	No hits of at least 90% identity	88.13	Chloroflexi Herpetosiphonales Herpetosiphonaceae
OTU.541	4.49	30	No hits of at least 90% identity	84.23	Verrucomicrobia Spartobacteria Chthoniobacterales
OTU.5539	4.01	14	<i>Devosia subaequoris</i>	98.17	Proteobacteria Alphaproteobacteria Rhizobiales

Table S1 – continued from previous page

OTU ID	Fold change	Day	Top BLAST hits	BLAST %ID	Phylum;Class;Order
OTU.573	3.03	30	<i>Adhaeribacter aerophilus</i>	92.76	<i>Bacteroidetes Cytophagia Cytophagales</i>
OTU.6	3.62	7	<i>Cellvibrio fulvus</i>	100.0	<i>Proteobacteria Gammaproteobacteria Pseudomonadales</i>
OTU.600	3.48	30	No hits of at least 90% identity	80.37	<i>Planctomycetes Planctomycetacia Planctomycetales</i>
OTU.6062	4.83	30	<i>Dokdonella sp. DC-3, Luteibacter rhizovicinus</i>	97.26	<i>Proteobacteria Gammaproteobacteria Xanthomonadales</i>
OTU.627	4.43	14	<i>Verrucomicrobiaceae bacterium DC2a-G7</i>	100.0	<i>Verrucomicrobia Verrucomicrobiae Verrucomicrobiales</i>
OTU.633	3.84	30	No hits of at least 90% identity	89.5	<i>Proteobacteria Deltaproteobacteria Myxococcales</i>
OTU.638	4.0	30	<i>Luteolibacter sp. CCTCC AB 2010415, Luteolibacter algae</i>	93.61	<i>Verrucomicrobia Verrucomicrobiae Verrucomicrobiales</i>
OTU.64	4.31	14	No hits of at least 90% identity	89.5	<i>Chloroflexi Herpetosiphonales Herpetosiphonaceae</i>
OTU.663	3.63	30	<i>Pirellula staleyi DSM 6068</i>	90.87	<i>Planctomycetes Planctomycetacia Planctomycetales</i>
OTU.669	3.34	30	<i>Ohtaekwangia koreensis</i>	92.69	<i>Bacteroidetes Cytophagia Cytophagales</i>
OTU.670	2.87	30	<i>Adhaeribacter aerophilus</i>	91.78	<i>Bacteroidetes Cytophagia Cytophagales</i>
OTU.766	3.21	14	<i>Devosia insulae</i>	99.54	<i>Proteobacteria Alphaproteobacteria Rhizobiales</i>
OTU.83	5.61	14	<i>Luteolibacter sp. CCTCC AB 2010415</i>	97.72	<i>Verrucomicrobia Verrucomicrobiae Verrucomicrobiales</i>
OTU.862	5.87	14	<i>Allokutzneria albata</i>	100.0	<i>Actinobacteria Pseudonocardiales Pseudonocardiaceae</i>
OTU.899	2.28	30	<i>Enhygromyxa salina</i>	97.72	<i>Proteobacteria Deltaproteobacteria Myxococcales</i>
OTU.90	2.94	14	<i>Sphingopyxis panaciterrae, Sphingopyxis chilensis, Sphingopyxis sp. BZ30, Sphingomonas sp.</i>	100.0	<i>Proteobacteria Alphaproteobacteria Sphingomonadales</i>
OTU.900	4.87	14	<i>Brevundimonas vesicularis, Brevundimonas nasdae</i>	100.0	<i>Proteobacteria Alphaproteobacteria Caulobacterales</i>
OTU.971	3.68	30	No hits of at least 90% identity	78.57	<i>Chloroflexi Anaerolineae Anaerolineales</i>
OTU.98	3.68	14	No hits of at least 90% identity	88.18	<i>Chloroflexi Herpetosiphonales Herpetosiphonaceae</i>
OTU.982	4.47	14	<i>Devosia neptuniae</i>	100.0	<i>Proteobacteria Alphaproteobacteria Rhizobiales</i>

<sup>a</sup> Maximum observed  $\log_2$  of fold change.<sup>b</sup> Day of maximum fold change.

Table S2:  $^{13}\text{C}$ -xylose responders BLAST against Living Tree Project

OTU ID	Fold change <sup>a</sup>	Day <sup>b</sup>	Top BLAST hits	BLAST %ID	Phylum;Class;Order
OTU.1040	4.78	1	<i>Paenibacillus daejeonensis</i>	100.0	<i>Firmicutes Bacilli Bacillales</i>
OTU.1069	3.85	1	<i>Paenibacillus terrigena</i>	100.0	<i>Firmicutes Bacilli Bacillales</i>
OTU.107	2.25	3	<i>Flavobacterium sp. 15C3</i> , <i>Flavobacterium banpakuense</i>	99.54	<i>Bacteroidetes Flavobacteria Flavobacteriales</i>
OTU.11	5.25	7	<i>Stenotrophomonas pavanii</i> , <i>Stenotrophomonas maltophilia</i> , <i>Pseudomonas geniculata</i>	99.54	<i>Proteobacteria Gammaproteobacteria Xanthomonadales</i>
OTU.131	3.07	3	<i>Flavobacterium fluvii</i> , <i>Flavobacterium bacterium HMD1033</i> , <i>Flavobacterium sp. HMD1001</i>	100.0	<i>Bacteroidetes Flavobacteria Flavobacteriales</i>
OTU.14	3.92	3	<i>Flavobacterium oncorhynchi</i> , <i>Flavobacterium glycines</i> , <i>Flavobacterium succinicans</i>	99.09	<i>Bacteroidetes Flavobacteria Flavobacteriales</i>
OTU.150	3.08	14	No hits of at least 90% identity	86.76	<i>Planctomycetes Planctomycetacia Planctomycetales</i>
OTU.159	3.16	3	<i>Flavobacterium hibernum</i>	98.17	<i>Bacteroidetes Flavobacteria Flavobacteriales</i>
OTU.165	2.38	3	<i>Rhizobium skieniewicense</i> , <i>Rhizobium vignae</i> , <i>Rhizobium larrymoorei</i> , <i>Rhizobium alkalisolii</i> , <i>Rhizobium galegae</i> , <i>Rhizobium huautlense</i>	100.0	<i>Proteobacteria Alphaproteobacteria Rhizobiales</i>
OTU.183	3.31	3	No hits of at least 90% identity	89.5	<i>Bacteroidetes Sphingobacteriia Sphingobacteriales</i>
OTU.19	2.14	7	<i>Rhizobium alamii</i> , <i>Rhizobium mesosinicum</i> , <i>Rhizobium mongolense</i> , <i>Arthrobacter viscosus</i> , <i>Rhizobium sullae</i> , <i>Rhizobium yanglingense</i> , <i>Rhizobium loessense</i>	99.54	<i>Proteobacteria Alphaproteobacteria Rhizobiales</i>
OTU.2040	2.91	1	<i>Paenibacillus pectinilyticus</i>	100.0	<i>Firmicutes Bacilli Bacillales</i>
OTU.22	2.8	7	<i>Paracoccus sp. NB88</i>	99.09	<i>Proteobacteria Alphaproteobacteria Rhodobacterales</i>
OTU.2379	3.1	3	<i>Flavobacterium pectinovorum</i> , <i>Flavobacterium sp. CS100</i>	97.72	<i>Bacteroidetes Flavobacteria Flavobacteriales</i>
OTU.24	2.81	7	<i>Cellulomonas aerilata</i> , <i>Cellulomonas humilata</i> , <i>Cellulomonas terrae</i> , <i>Cellulomonas soli</i> , <i>Cellulomonas xylinilytica</i>	100.0	<i>Actinobacteria Micrococcales Cellulomonadaceae</i>
OTU.241	3.38	3	No hits of at least 90% identity	87.73	<i>Verrucomicrobia Spartobacteria Chthoniobacterales</i>
OTU.244	3.08	7	<i>Cellulosimicrobium funkei</i> , <i>Cellulosimicrobium terreum</i>	100.0	<i>Actinobacteria Micrococcales Promicromonosporaceae</i>
OTU.252	3.34	7	<i>Promicromonospora thailandica</i>	100.0	<i>Actinobacteria Micrococcales Promicromonosporaceae</i>
OTU.267	4.97	1	<i>Paenibacillus pabuli</i> , <i>Paenibacillus tundrae</i> , <i>Paenibacillus taichungensis</i> , <i>Paenibacillus xylohexedens</i> , <i>Paenibacillus xylinilyticus</i>	100.0	<i>Firmicutes Bacilli Bacillales</i>
OTU.277	3.52	3	<i>Solibius ginsengiterrae</i>	95.43	<i>Bacteroidetes Sphingobacteriia Sphingobacteriales</i>

Table S2 – continued from previous page

OTU ID	Fold change	Day	Top BLAST hits	BLAST %ID	Phylum;Class;Order
OTU.290	3.59	1	<i>Pantoea spp.</i> , <i>Klugvera spp.</i> , <i>Klebsiella spp.</i> , <i>Erwinia spp.</i> , <i>Enterobacter spp.</i> , <i>Buttiauxella spp.</i>	100.0	Proteobacteria Gammaproteobacteria Enterobacterales
OTU.3	2.61	1	[ <i>Brevibacterium</i> ] <i>frigoritolerans</i> , <i>Bacillus sp.</i> LMG 20238, <i>Bacillus coahuilensis</i> m4-4, <i>Bacillus simplex</i>	100.0	Firmicutes Bacilli Bacillales
OTU.319	3.98	1	<i>Paenibacillus xinjiangensis</i>	97.25	Firmicutes Bacilli Bacillales
OTU.32	3.0	3	<i>Sandaracinus amyloyticus</i>	94.98	Proteobacteria Deltaproteobacteria Myxococcales
OTU.335	2.53	1	<i>Paenibacillus thailandensis</i>	98.17	Firmicutes Bacilli Bacillales
OTU.346	3.44	3	<i>Pseudoduganella violaceinigra</i>	99.54	Proteobacteria Betaproteobacteria Burkholderiales
OTU.3507	2.36	1	<i>Bacillus spp.</i>	98.63	Firmicutes Bacilli Bacillales
OTU.3540	2.52	3	<i>Flavobacterium terrigena</i>	99.54	Bacteroidetes Flavobacteria Flavobacterales
OTU.360	2.98	3	<i>Flavisolibacter ginsengisoli</i>	95.0	Bacteroidetes Sphingobacteriia Sphingobacterales
OTU.369	5.05	1	<i>Paenibacillus sp.</i> D75, <i>Paenibacillus glycansilyticus</i>	100.0	Firmicutes Bacilli Bacillales
OTU.37	2.68	7	<i>Phycicola gilvus</i> , <i>Microterricola viridarii</i> , <i>Frigeribacterium faeni</i> , <i>Frondihabitans sp.</i> RS-15, <i>Frondihabitans australicus</i>	100.0	Actinobacteria Micrococcales Microbacteriaceae
OTU.394	4.06	1	<i>Paenibacillus pocheonensis</i>	100.0	Firmicutes Bacilli Bacillales
OTU.4	2.84	7	<i>Agromyces ramosus</i>	100.0	Actinobacteria Micrococcales Microbacteriaceae
OTU.4446	3.49	7	<i>Catenuloplanes niger</i> , <i>Catenuloplanes castaneus</i> , <i>Catenuloplanes atrovinosus</i> , <i>Catenuloplanes crispus</i> , <i>Catenuloplanes nepalensis</i> , <i>Catenuloplanes japonicus</i>	97.72	Actinobacteria Frankiales Nakamurellaceae
OTU.4743	2.24	1	<i>Lysinibacillus fusiformis</i> , <i>Lysinibacillus sphaericus</i>	99.09	Firmicutes Bacilli Bacillales
OTU.48	2.99	1	<i>Aeromonas spp.</i>	100.0	Proteobacteria Gammaproteobacteria aaa34a10
OTU.5	3.69	7	<i>Delftia tsuruhatensis</i> , <i>Delftia lacustris</i>	100.0	Proteobacteria Betaproteobacteria Burkholderiales
OTU.5284	3.56	7	<i>Isopotericola nanjingensis</i> , <i>Isopotericola hypogaeus</i> , <i>Isopotericola variabilis</i>	98.63	Actinobacteria Micrococcales Promicromonosporaceae
OTU.5603	3.96	1	<i>Paenibacillus uliginis</i>	100.0	Firmicutes Bacilli Bacillales
OTU.57	4.39	1	<i>Paenibacillus castaneae</i>	98.62	Firmicutes Bacilli Bacillales
OTU.5906	3.16	3	<i>Terrimonas sp.</i> M-8	96.8	Bacteroidetes Sphingobacteriia Sphingobacterales
OTU.6	3.24	3	<i>Cellvibrio fulvus</i>	100.0	Proteobacteria Gammaproteobacteria Pseudomonadales
OTU.62	2.57	7	<i>Nakamurella flava</i>	100.0	Actinobacteria Frankiales Nakamurellaceae

Table S2 – continued from previous page

OTU ID	Fold change	Day	Top BLAST hits	BLAST %ID	Phylum;Class;Order
OTU.6203	3.32	3	<i>Flavobacterium granuli</i> , <i>Flavobacterium glaciei</i>	100.0	<i>Bacteroidetes Flavobacteria Flavobacteriales</i>
OTU.68	3.74	7	<i>Shigella flexneri</i> , <i>Escherichia fergusonii</i> , <i>Escherichia coli</i> , <i>Shigella sonnei</i>	100.0	<i>Proteobacteria Gammaproteobacteria Enterobacteriales</i>
OTU.760	2.89	3	<i>Dyadobacter hamtensis</i>	98.63	<i>Bacteroidetes Cytophagia Cytophagales</i>
OTU.8	2.26	1	<i>Bacillus niaci</i>	100.0	<i>Firmicutes Bacilli Bacillales</i>
OTU.843	3.62	1	<i>Paenibacillus agaragedens</i>	100.0	<i>Firmicutes Bacilli Bacillales</i>
OTU.9	2.04	1	<i>Bacillus megaterium</i> , <i>Bacillus flexus</i>	100.0	<i>Firmicutes Bacilli Bacillales</i>

<sup>a</sup> Maximum observed  $\log_2$  of fold change.<sup>b</sup> Day of maximum fold change.